Efficiency improvement of a bearingless motor with powder iron core

D. Kanehara*, J. Asama*, T. Oiwa, A. Chiba** (*Shizuoka University, Japan **Tokyo Institute of Technology, Japan)

Introduction

Bearingless motor

☐A motor which combines magnetic bearing function and rotation in the same unit

◎ No wear particles, Lubricant-free

☐Application : Chemical pumps, Blood pumps, etc

Previous research

☐Proposed a compact bearingless motor (fig.1)

☐Succeeded in stable suspension and rotation

☐Problem : Motor loss is large ⇒ Low efficiency (fig.3)

Research objective

☐Improvement of efficiency with powder iron core

Proposed bearingless motor

Structure

☐Rotor : Two iron disks (with PM) and a PM ring

☐Stator : C-shape ⇒ Reduction motor height

☐Two kind of windings

: Suspension and motor are combined

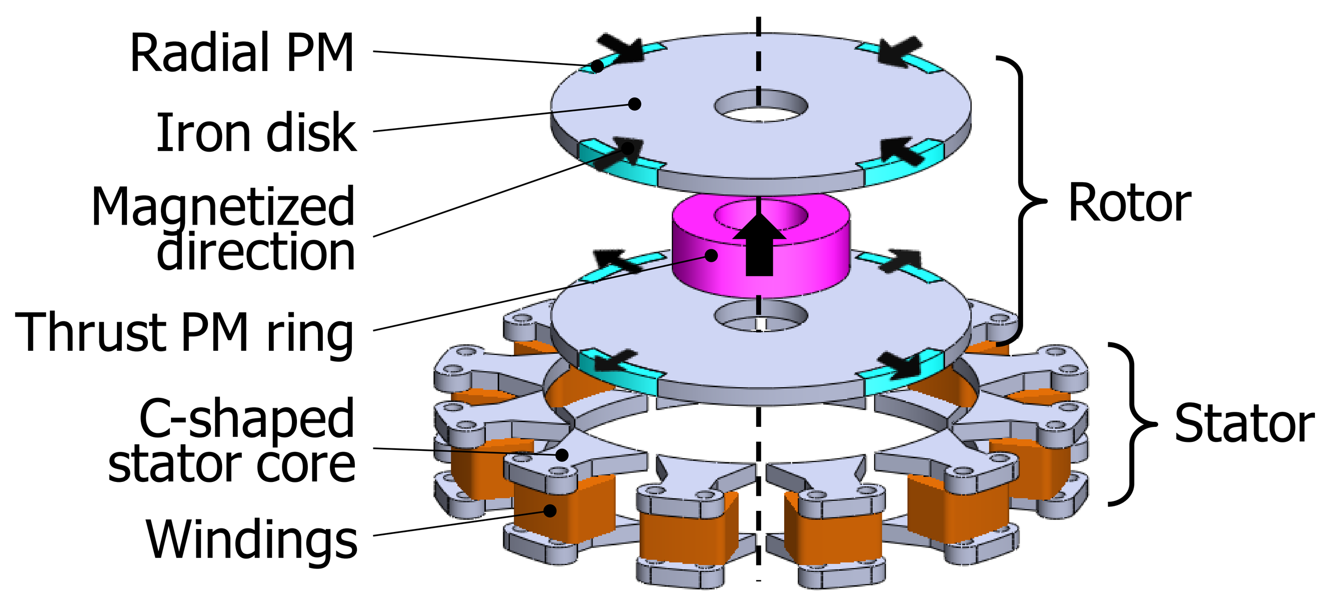

Fig.1 Proposed structure

Magnet suspension principle

☐Radial direction : Suspension force is generated by superposition of PM flux and suspension flux

☐Radial position (suspension force) is actively regulated

☐Axial/tilting direction : Passively stable with magnetic attractive force

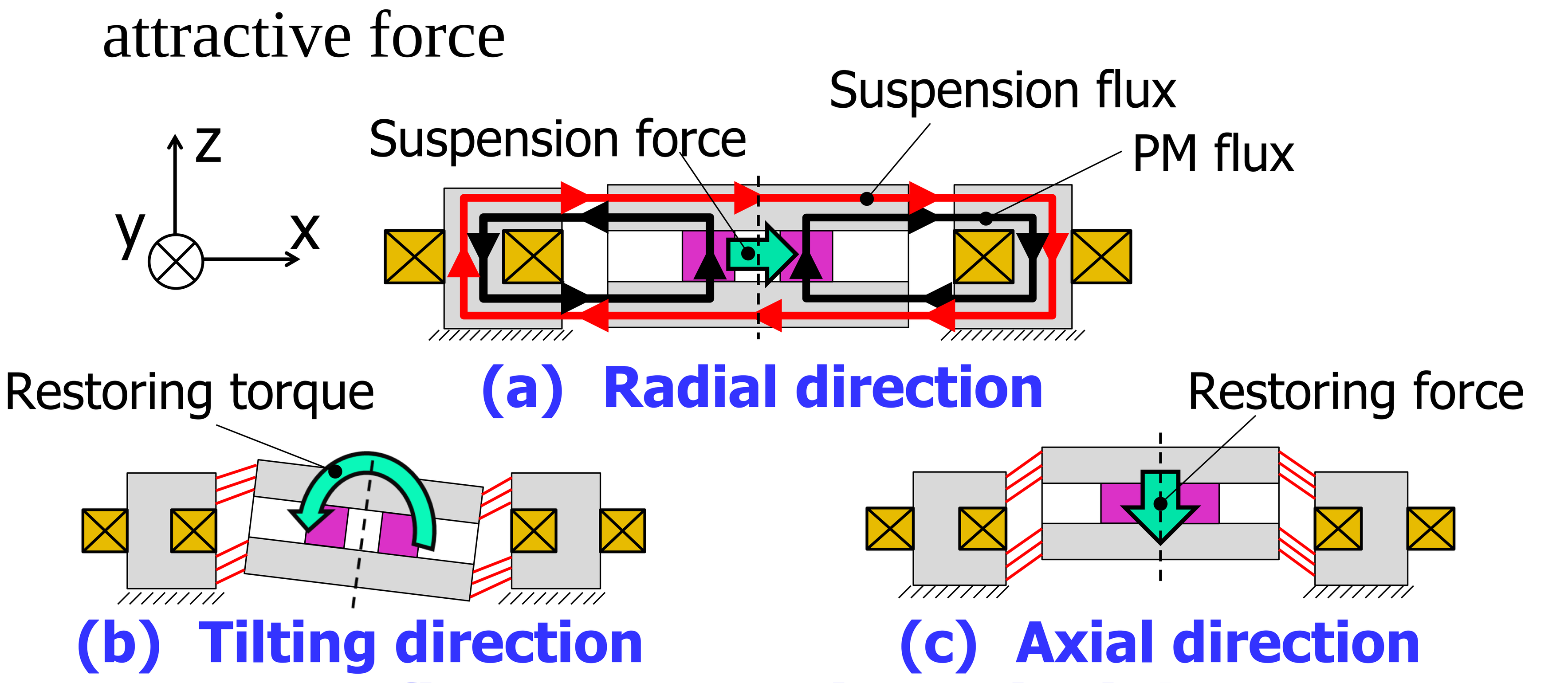

fig.2 Suspension principle

Test machine loss (with bulk core)

Power consumption with no load

☐Motor loss is 70% or more of total loss

☐Iron loss is 60% of motor loss ⇐ Eddy current

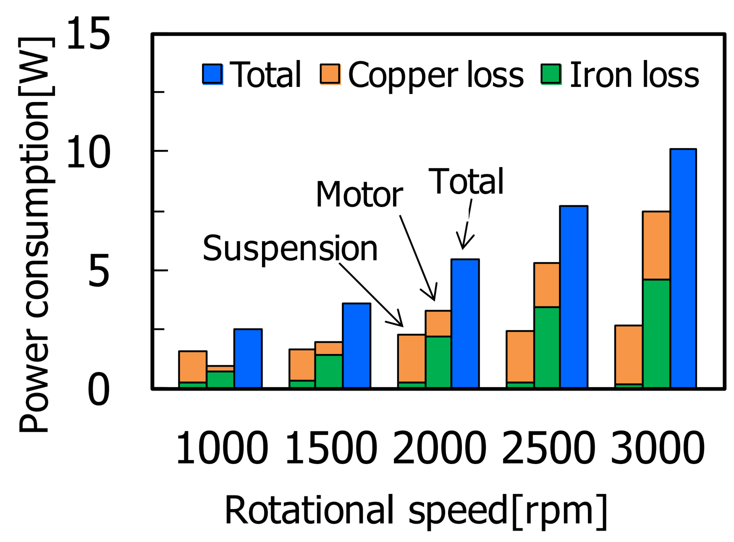

No load | Frictionless

$$P_{total} = P_{output} + P_{mech} + P_{copper} + P_{iron}$$

Increase

$$P_{iron} = P_{hysteresis} + P_{eddy\ current}$$

fig.3 Power consumption

Iron loss reduction

Powder iron core

☐Powder iron core is material which compresses insulated iron powder

☐ High electrical resistance ⇒ Reduced eddy current
⇒ Reduced iron loss

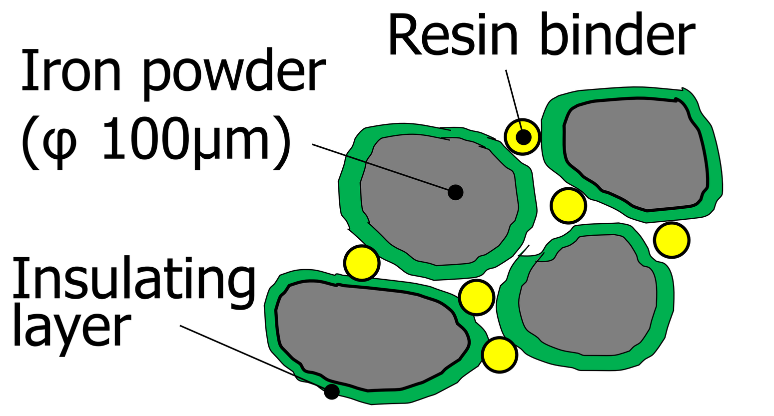

× Low permeability than bulk
⇒ Torque and force are reduced?
⇒ Investigation of motor performance with powder iron core

fig.4 Powder iron core

Test machine with powder iron core

☐Use powder iron core for stator core of proposed bearingless motor

☐Stator core is molded with epoxy resin
⇐ Because powder iron core is very brittle

☐Rotor motion range in radial direction is ±0.25mm

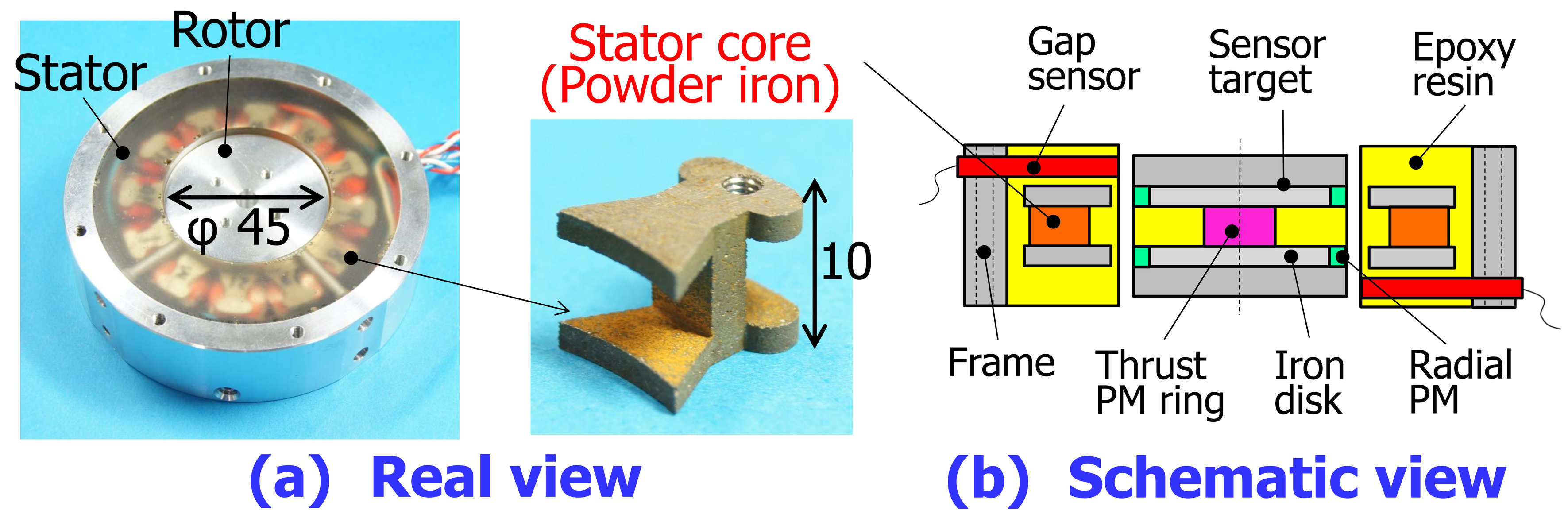

fig.5 Fabricated test machine

Powder iron core performance

Power consumption with no load

☐Total : 74% reduction (Motor loss reduction is large)

☐Iron loss : 85% reduction ⇒ Eddy current is reduced

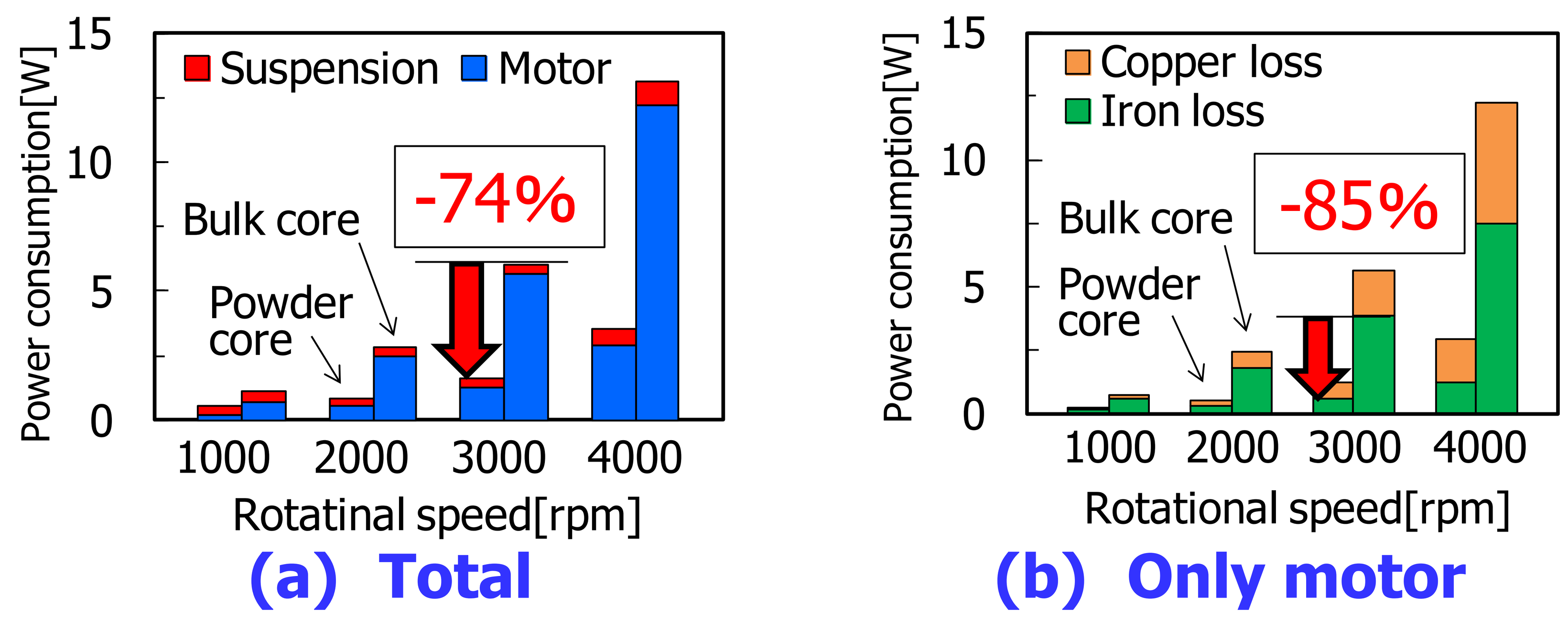

fig.6 Measured power consumption

Torque and Efficiency

☐Torque (k_T[mNm/A]) at 3000rpm : Powder ＞ Bulk
⇐ Eddy current works as brakes

☐Efficiency : 25% improvement (at 3000rpm)

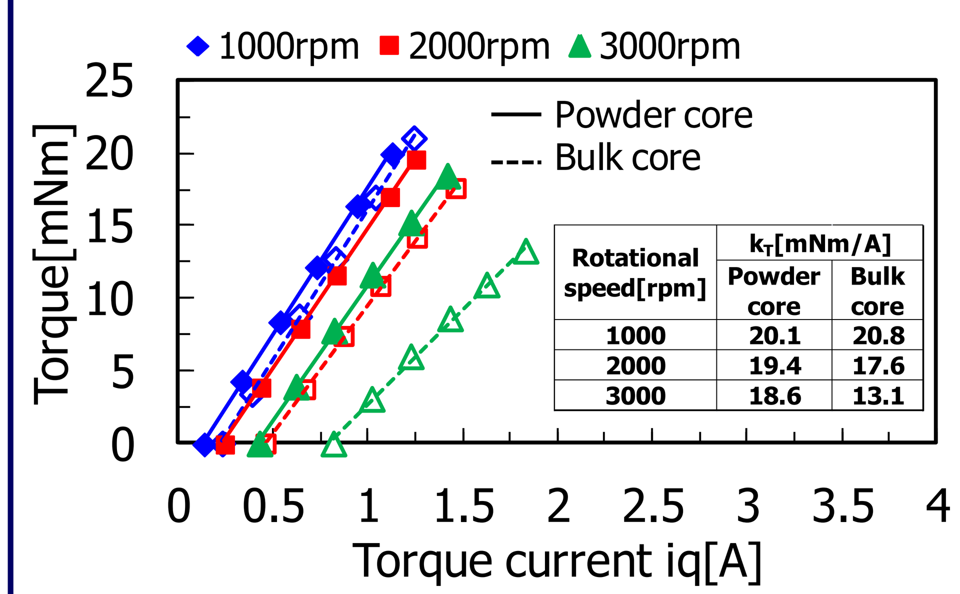

Rotational speed[rpm]	k_T[mNm/A] Powder core	k_T[mNm/A] Bulk core
1000	20.1	20.8
2000	19.4	17.6
3000	18.6	13.1

fig.7 Measured torque

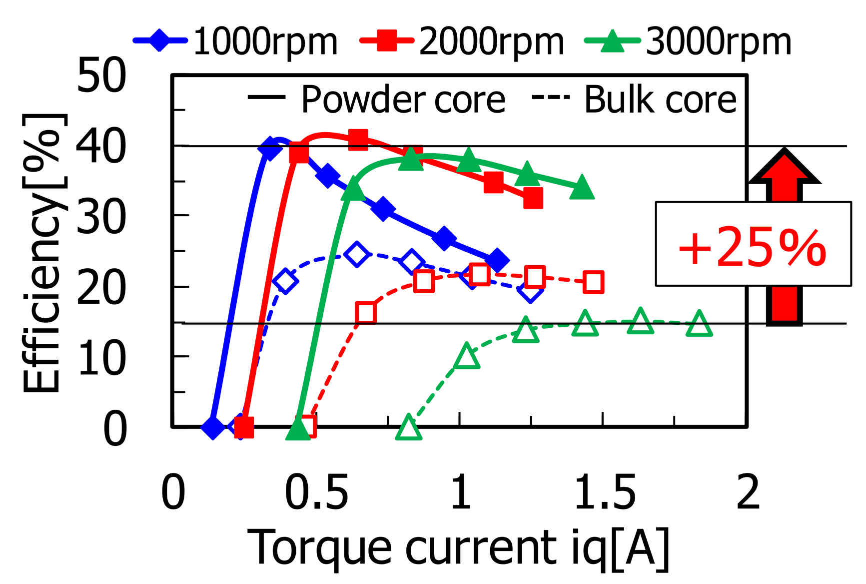

fig.8 Efficiency

Conclusion

☐It is effective to use powder iron core for proposed bearingless motor to improve efficiency

Force Interference Reduction with Winding Configuration in a Homo-polar Bearingless Motor

Y. Yamamoto[1], J. Asama[1],
[1] Shizuoka University, Japan.

Background and Objective

Final Goal of Research

Realization of **precise positioning** bearingless motor

Application possibility: Micro endmilll cutting

Problem of conventional cutting { axial runout; Heterogeneous cutting force

Bearingless motor

Position of endmill, Cutting force } Measurement and control ⇒ Realization of Precision cutting

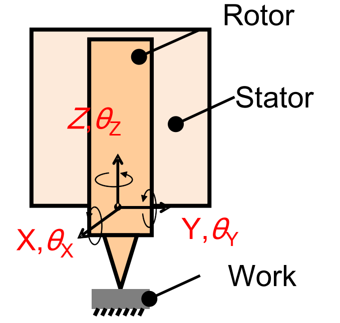

Fig.1 Concept of application

Proposed Structure

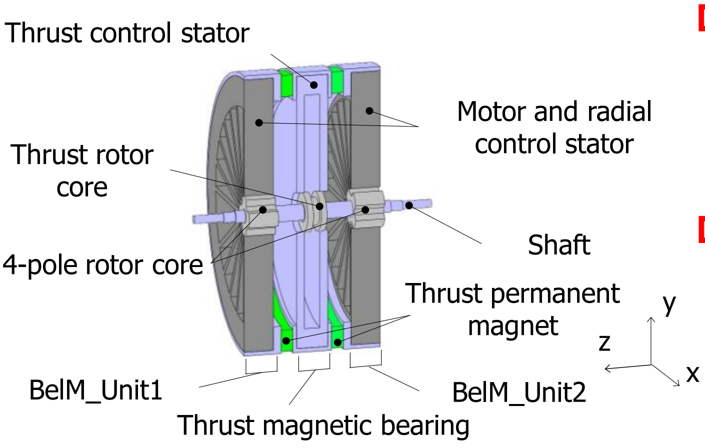

Fig.2 Proposed structure of homo-polar bearingless motor

- ☐ 8-pole homo-polar bearingless motor
  Permanent magnet-free (on rotor)

  Realization of Robust rotor

- ☐ 5 DOF control
  - BelM_Unit1 and BelM_Unit2: X, Y, θ_X, θ_Y
  - Thrust control bearing(TMB): Z
- ☐ Distributed winding
- ☐ 24 slots

  } Sine wave MMF

Principle of Radial Suspension Force and Direction Error

☐ Undersirable Force Interference (Fig.3)

(a) At a symmetrical position

Suspension force F_x

(b) At an asymmetrical positior

Suspension force F_x and F_{yx}

Affects the control system

Error angle $\theta_e = \tan^{-1}(\frac{F_{yx}}{F_x})$

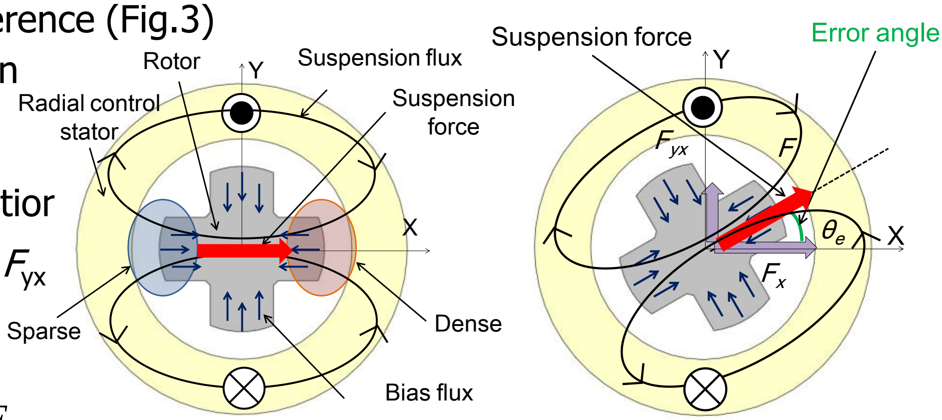

(a) Symmetrical (b) Asymmetrical

Fig.3 Principle of radial suspension force

Objective of This Presentation

Investigation of the optimal two-pole suspension winding configuration for miniaturization of an error angle (Fig.3).

Investigation of Optimal Suspension Winding Configuration

Theoretical Calculation

☐ Calculated error angle θ_e

Calculated magnetomotive force distribution $A(\varphi)$ ➡ F_x, F_{yx}, θ_e

$$F_x = \frac{\mu_0 R l}{2 g_0^2} \int_{-\pi}^{\pi} A^2(\phi)\cos(\phi)d\phi \qquad F_{yx} = \frac{\mu_0 R l}{2 g_0^2} \int_{-\pi}^{\pi} A^2(\phi)\sin(\phi)d\phi$$

μ_0: the permeability of free space
g_0: the air gap length
R: the mean air-gap radius
l: the stack length

☐ Single-layer winding model

Slot No.2,3: 1 turn
No.1,4: M turn
(M=0, 0.1, 0.2, …, 0.9, 1)

U-phase	1 A
V-phase	-0.5 A
W-phase	-0.5 A

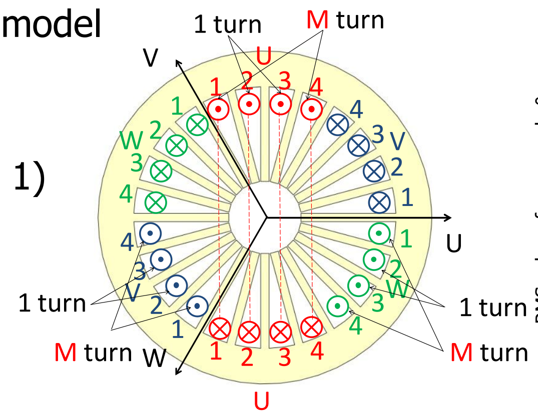

Fig.4 Single-layer winding (Model 1)

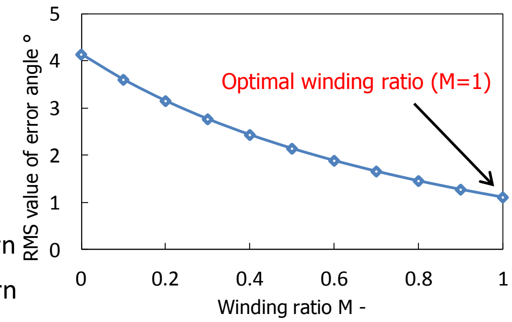

Fig.5 RMS value of error angle

☐ Double-layer winding model (Model 2)

Slot No.1~4: 1 turn
No.5,6: K turn
No.7,8: L turn
(K,L=0, 0.1, 0.2, …, 0.9, 1)

U-phase	1 A
V-phase	-0.5 A
W-phase	-0.5 A

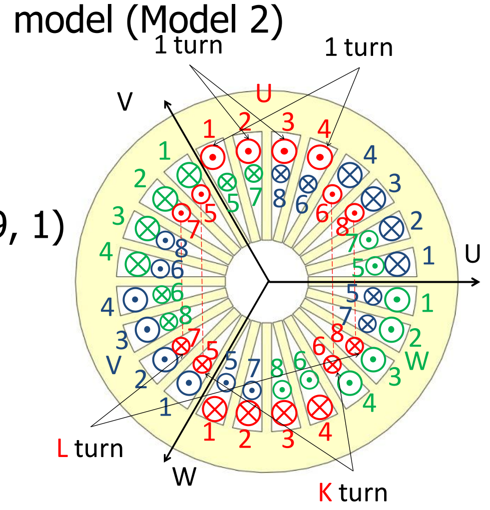

Fig.6 Double-layer winding (Model 2)

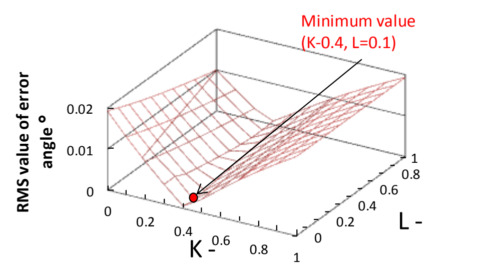

Fig.7 RMS value of error angle

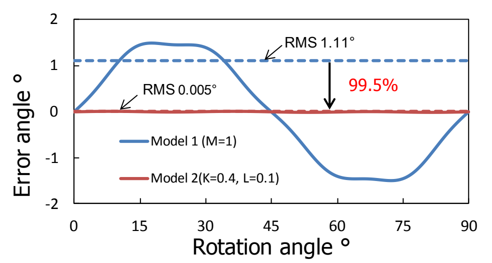

Fig.8 Comparison of Model 1 and Model 2

➡ RMS value of Model 2: 95.5% decreased against RMS value of Model 1

3D-FEM Analysis

☐ Analyze error angle θ_e

⬇

Certified validity of theoretical calculation

Table.1 RMS value of Theoretical calculation and FEM analysis

	Calculation	FEM
Model 1	1.11°	2.22°
Model 2	0.005°	0.300°

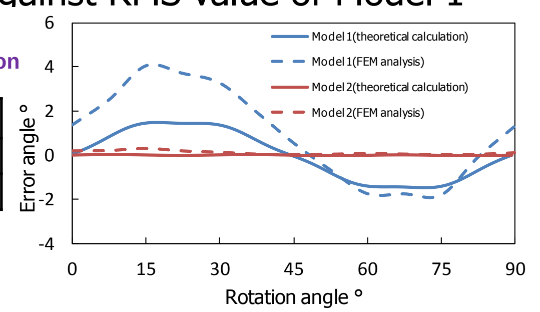

Fig.9 Comparison of theoretical calculation and FEM analysis

Conclusions

☐ Suspension winding configuration of Model 2 is optimal.
☐ 3D-FEM analysis results agree well with theoretical calculated results.
☐ Production test model in near future.

Design and Test Results of a One-DOF Actively Positioned Bearingless Motor

D.Watanabe*, J.Asama*, T.Oiwa*, A.Chiba**
*Shizuoka University, Japan **Tokyo Institute of Technology, Japan

Introduction

One-DOF actively positioned magnetic bearing motor

- Position control : Z direction
  ⇨ One-DOF actively positioned
- Required number of inverter
  - One single-phase inverter for magnetic bearing
  - One three-phase inverter for motor
  ⇨ ×Large size

(Fig.1)

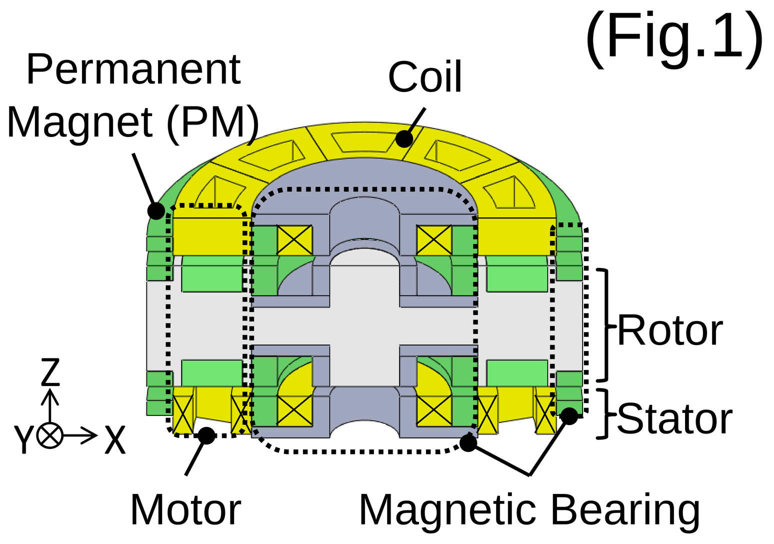

Fig.1 One-DOF actively positioned magnetic bearing motor (Reference:Tokyo Institute of Technology)

Magnetic bearing + Motor

Study objective

- Realize of one-DOF actively positioned bearingless motor only one three-phase inverter.

Configuration & Drive Principle

Configuration (Fig.2)

- One three-phase inverter
  ⇨ ○Small size
- 6-pole, 9-slot
- Coreless motor

Application: Cooling fan

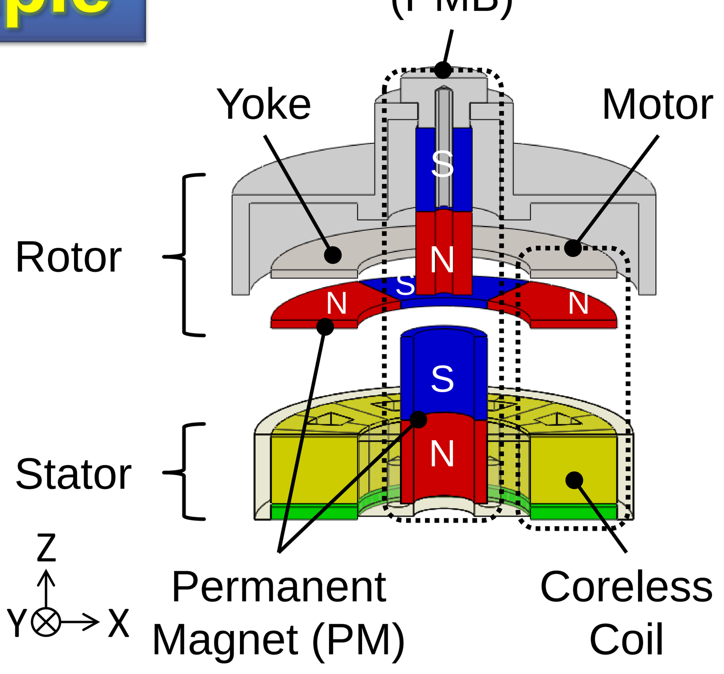

Fig.2 Proposed model

Position control & Rotation (Fig.3,4)

- Position control(Z) : d-axis current (i_d)
- Rotation(θ_z) : q-axis current (i_q)

Transformation formula

$$\begin{bmatrix} i_u \\ i_v \\ i_w \end{bmatrix} = \sqrt{\frac{2}{3}} \begin{bmatrix} 1 & 0 \\ -1/2 & \sqrt{3}/2 \\ -1/2 & -\sqrt{3}/2 \end{bmatrix} \begin{bmatrix} \cos\theta & -\sin\theta \\ \sin\theta & \cos\theta \end{bmatrix} \begin{bmatrix} i_d \\ i_q \end{bmatrix}$$

Position control

$$\text{If } \begin{pmatrix} i_d = 1 \\ i_q = 0 \\ \theta = 0 \end{pmatrix}, \text{ then } \begin{pmatrix} i_u = \sqrt{2/3} \\ i_v = -\sqrt{1/6} \\ i_w = -\sqrt{1/6} \end{pmatrix}$$

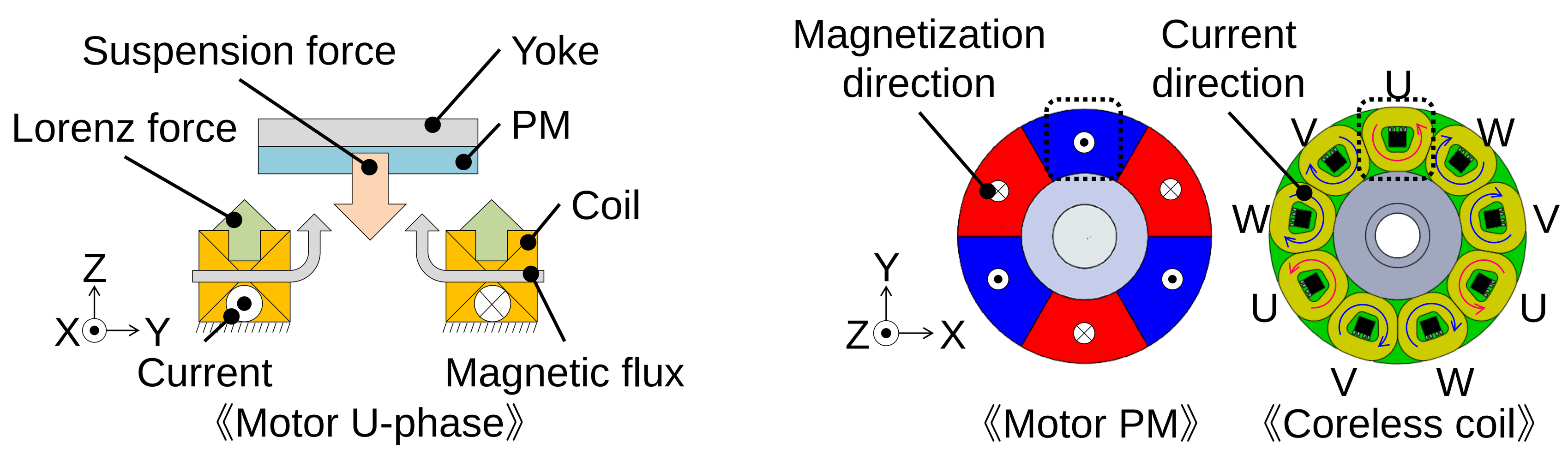

Fig.3 Principle of position control

Rotation

$$\text{If } \begin{pmatrix} i_d = 0 \\ i_q = 1 \\ \theta = 0 \end{pmatrix}, \text{ then } \begin{pmatrix} i_u = 0 \\ i_v = \sqrt{1/2} \\ i_w = -\sqrt{1/2} \end{pmatrix}$$

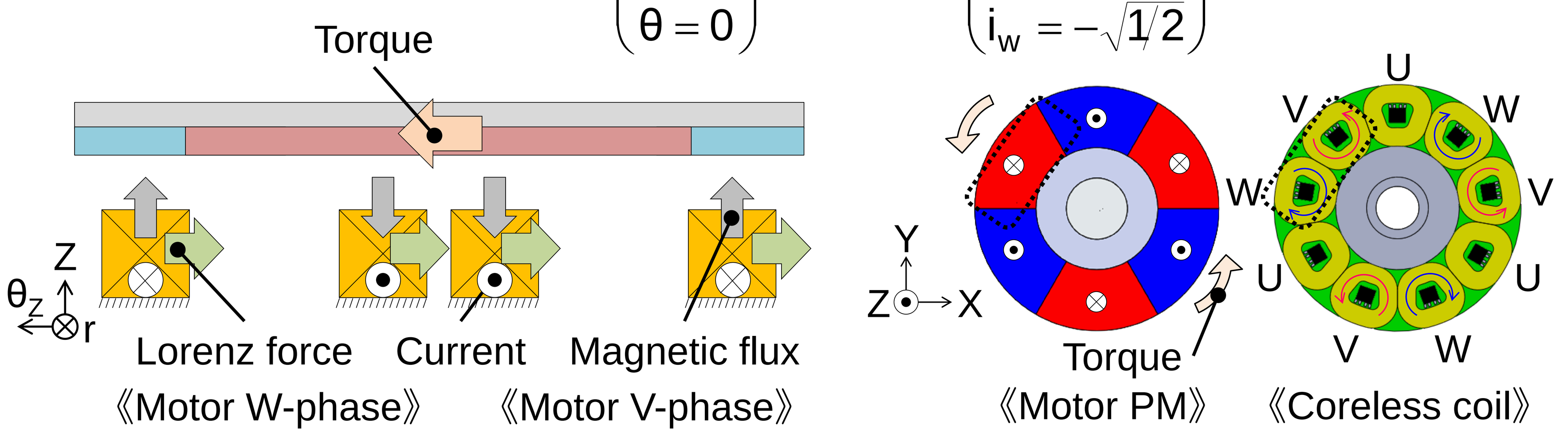

Fig.4 Principle of rotation

Passive suspension (Fig.5)

- Radial direction(X,Y) , Tilting direction(θ_X,θ_Y)

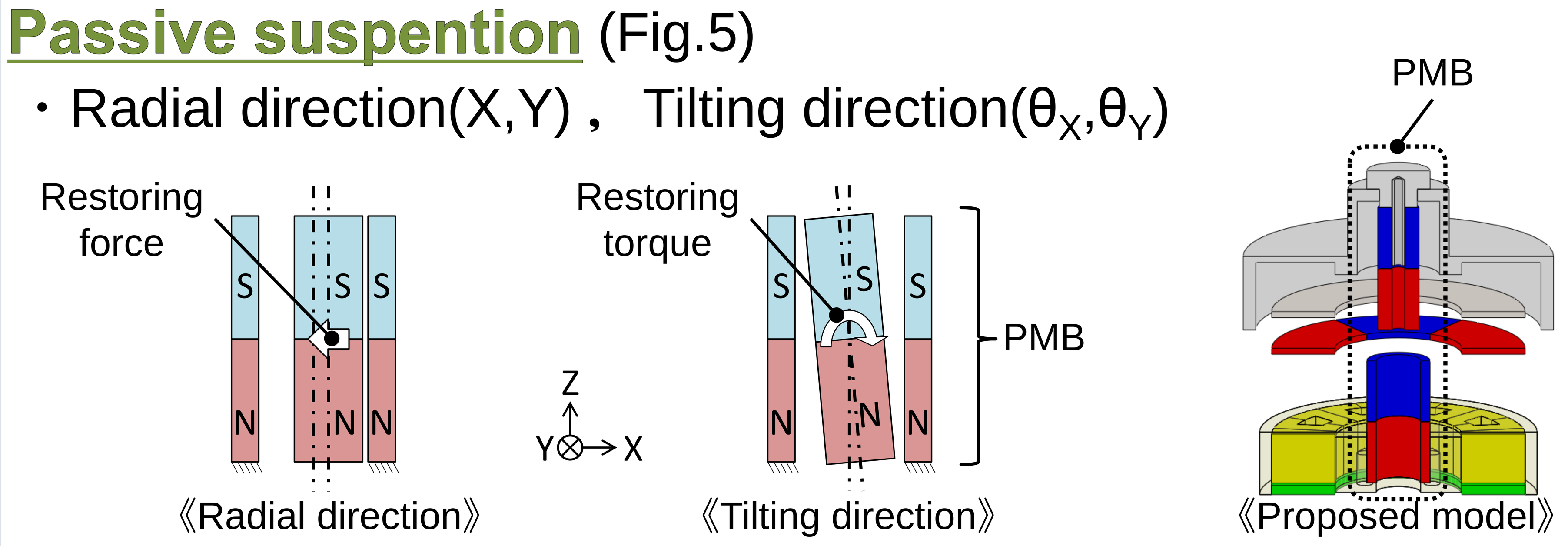

Fig.5 Principle of passive suspension

Electromagnetic Analysis

- Rated current : 0.25A
- Rated suspension force : 0.9N (Fig.6)
- Rated torque : 10mNm (Fig.7)

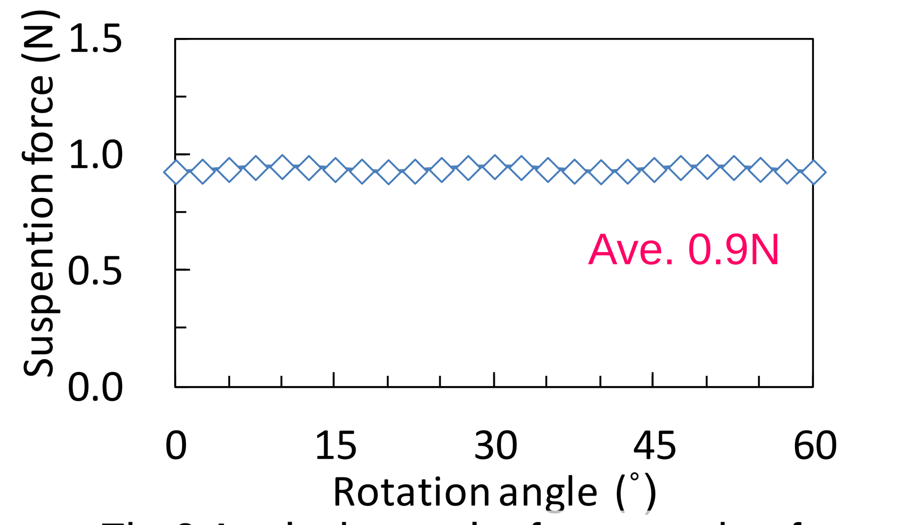

Fig.6 Analysis result of suspension force

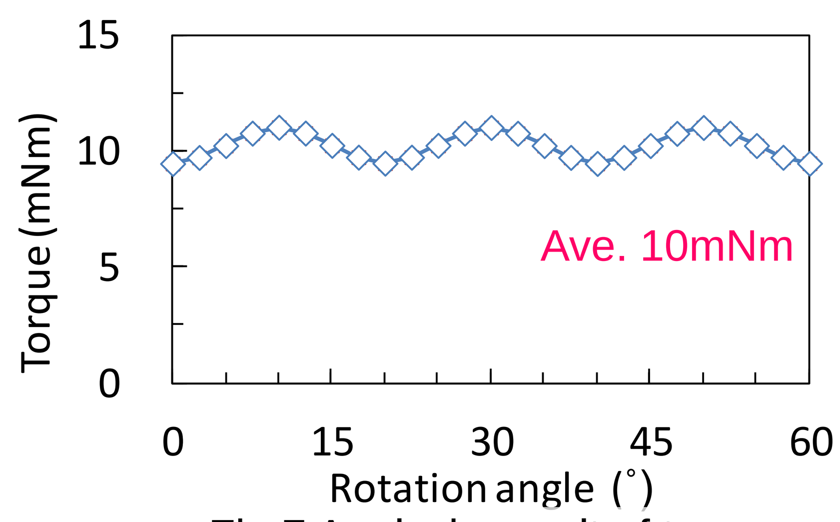

Fig.7 Analysis result of torque

Test Model

- Axial length : 26mm (Fig.8)
- Rotor diameter : 49mm (Fig.9)
- Magnetic gap : 1.0mm

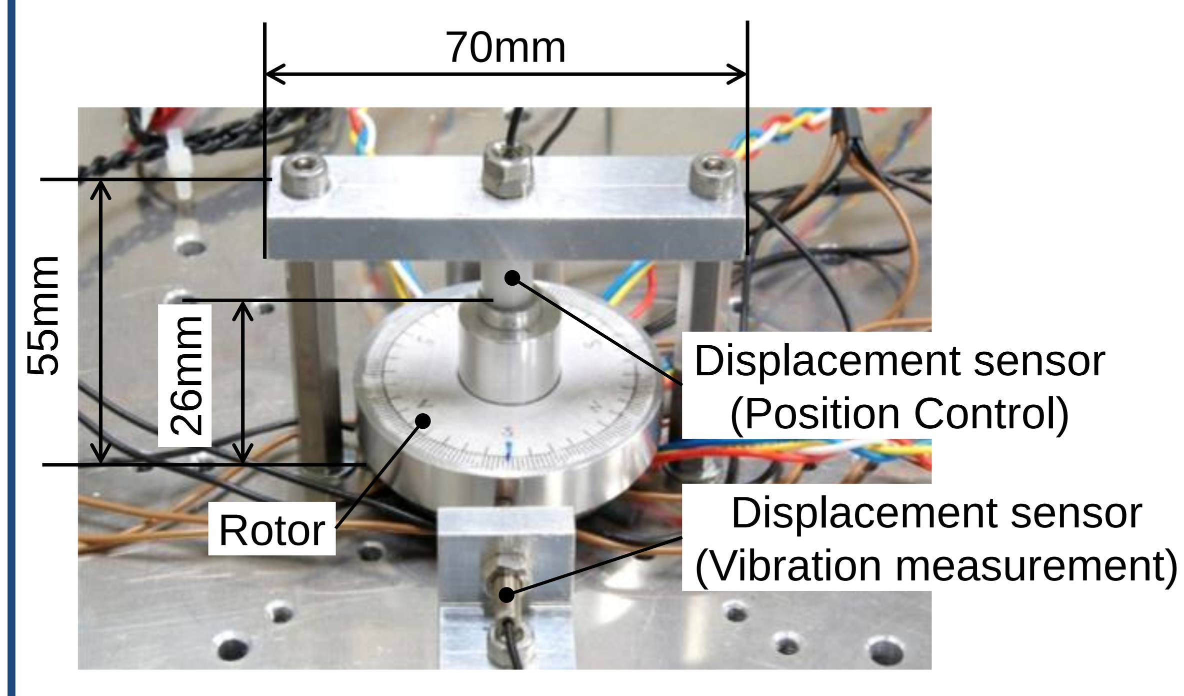

Fig.8 Prototype

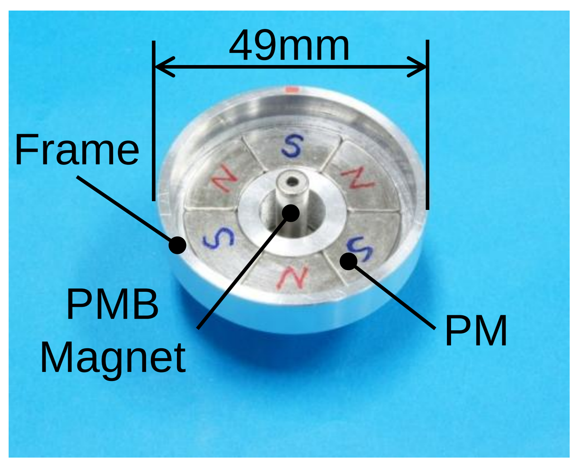

Fig.9 Rotor (Reverse)

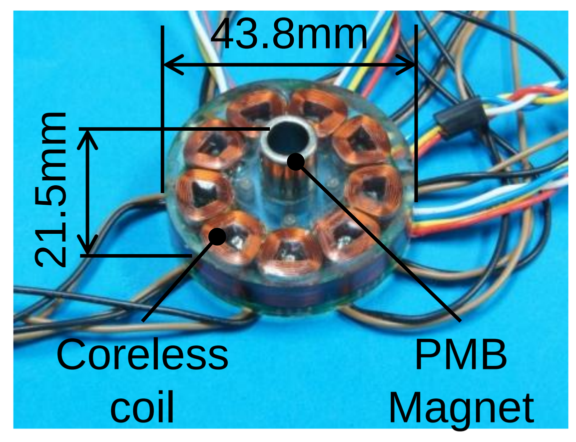

Fig.10 Stator

Drive test (No load)

Oscillation property (Fig.11,12)

- 2250rpm : Resonance of radial direction
- 3000rpm : Axial 4μm Tilting 4.9mrad
  Radial 0.07mm

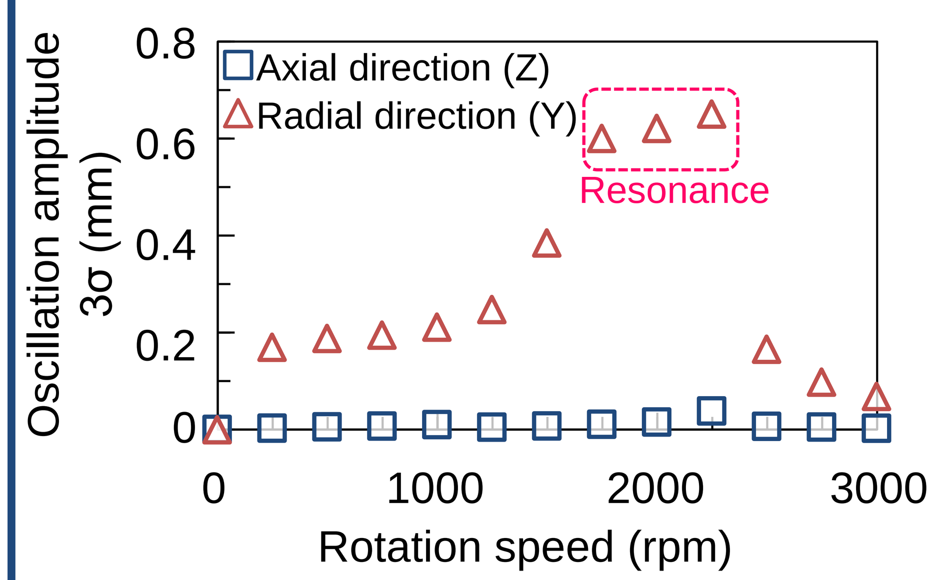

Fig.11 Radial and axial oscillation

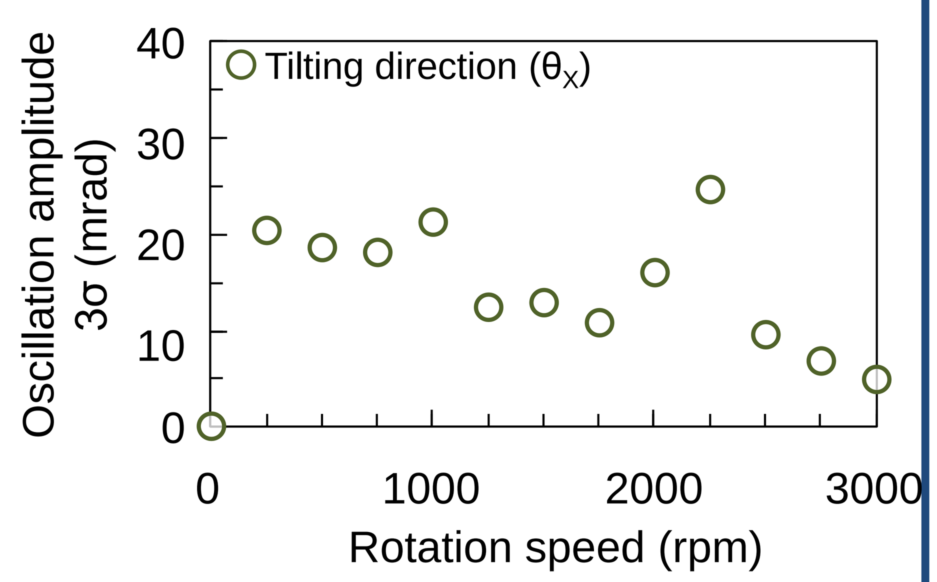

Fig.12 Tilting oscillation

Power consumption (Fig.13)

- 2250rpm
  Increase of oscillation
  ⇨ Friction loss, Copper loss — Increase
- 3000rpm : 0.14W

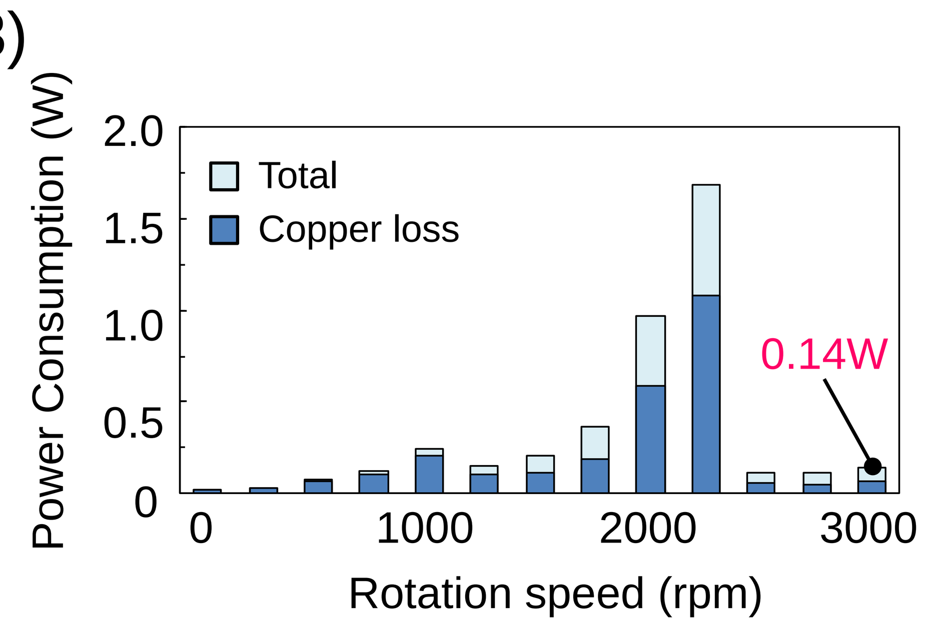

Fig.13 Power consumption

Conclusions

- One-DOF actively positioned bearingless motor for cooling fan is proposed.
- Rated suspension force is 0.9N, and rated torque is 10mNm.
- Axial, radial and tilting oscillation amplitude at 3000rpm are 4μm, 0.07mm, and 4.9mrad.

Fabrication of a three-phase votage source inverter and its drive

Y. Fujii, J. Asama
(Shizuoka University, Japan)

Introduction

Conventional AC motor control

□Supply of AC by commercial power
➡×Variable frequency , ×Variable voltage

Solution

Inverter control by PWM(pulse width modulation) control

□Variable voltage Variable frequency(VVVF) control
□Performance of inverter
➡Important fabrication of drive circuit

Goal of Research

Fabrication of three-phase voltage source inverter and its drive circuit

Outline of Inverter

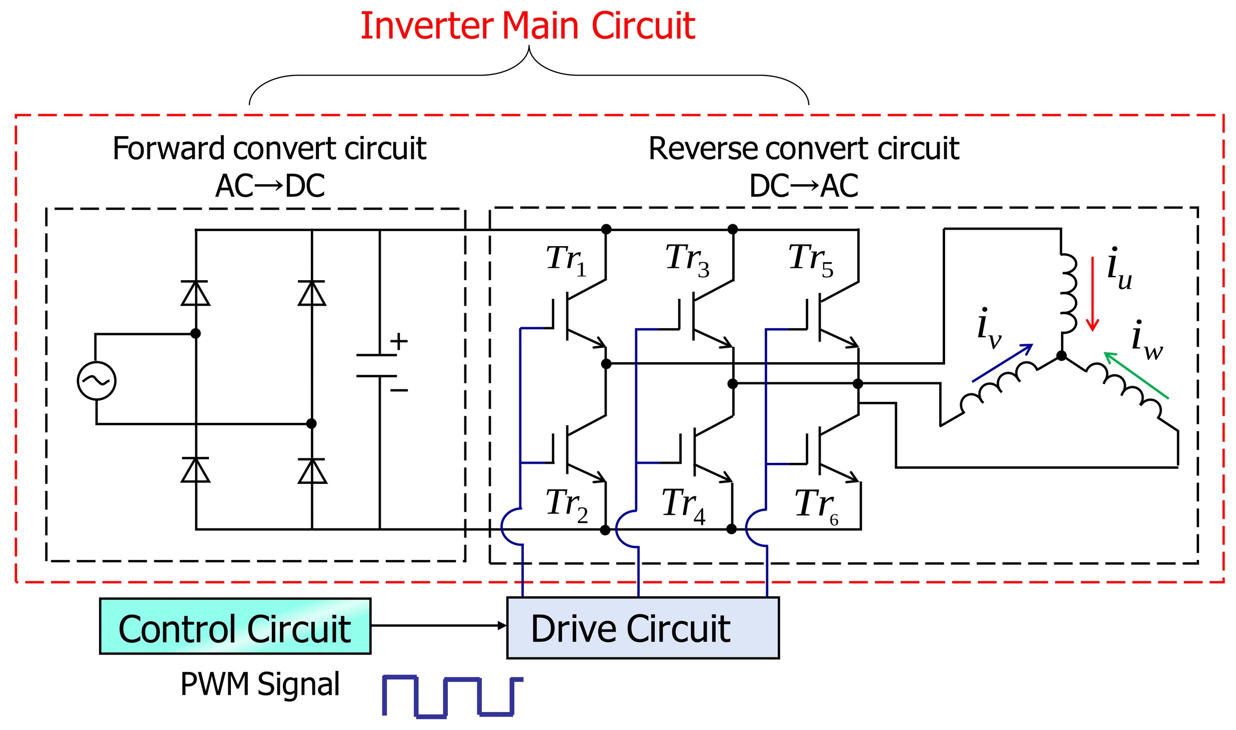

Fig.1. Outline of Inverter

Principle of behavior

□Forward Convert Circuit: rectifier from AC to DC
□Reverse Convert Circuit：from DC to AC
□Control Circuit :transmission of PWM signal
□Drive Circuit：switching semiconductor device

PWM(Pulse width modulation) Control

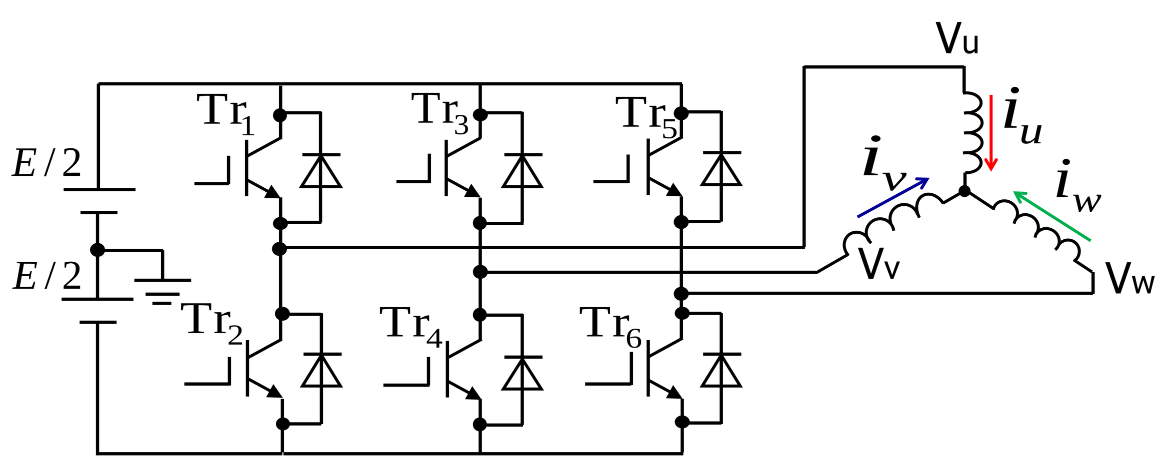

Fig.2.Variable Load voltage by switching

<Example>
focus on U-phase
□Tr1=ON➡Vu=E/2
□Tr2=ON➡Vu=-E/2

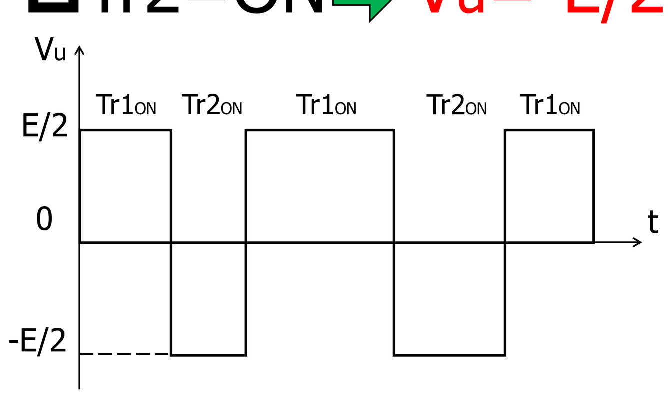

Approximation sinusoidal wave by PWM

□Comparison of carrier wave and modulation wave in control circuit
□In case of Modulation wave =Sinusoidal modulation wave
➡Output of approximation sinusoidal wave

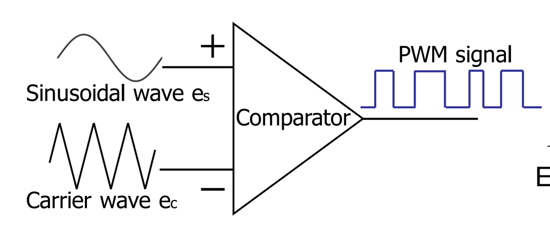

Fig.3. Carrier wave comparison

es>ec→Vu=E/2
es<ec→Vu=-E/2

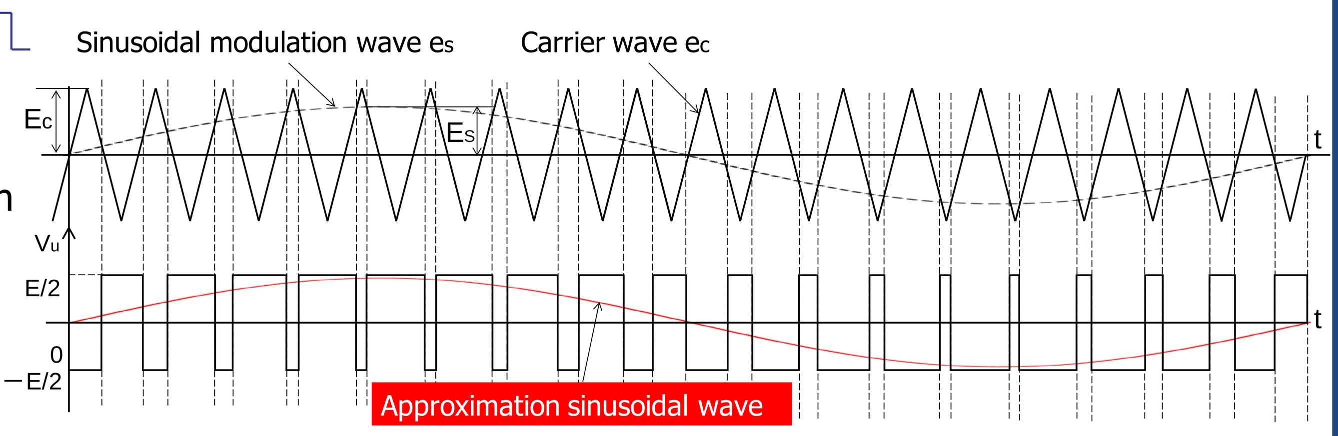

Fig.4. Principle of PWM control

Amplitude of modulation wave

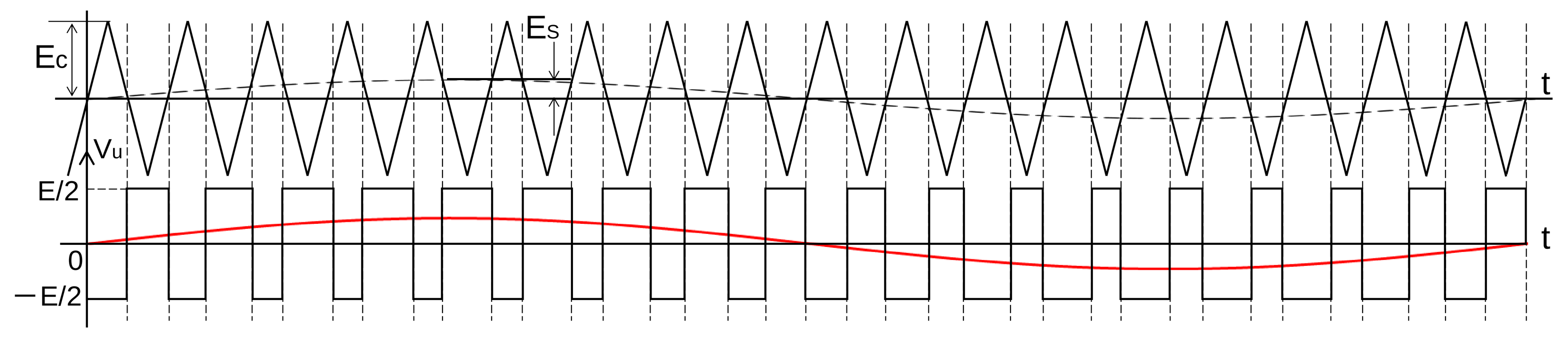

Fig.5. small amplitude of modulation wave

□Smaller amplitude of modulation wave than Fig.4.
□Amplitude of approximation sinusoidal wave
➡ Proportion to amplitude of modulation wave

Principle of Drive Circuit

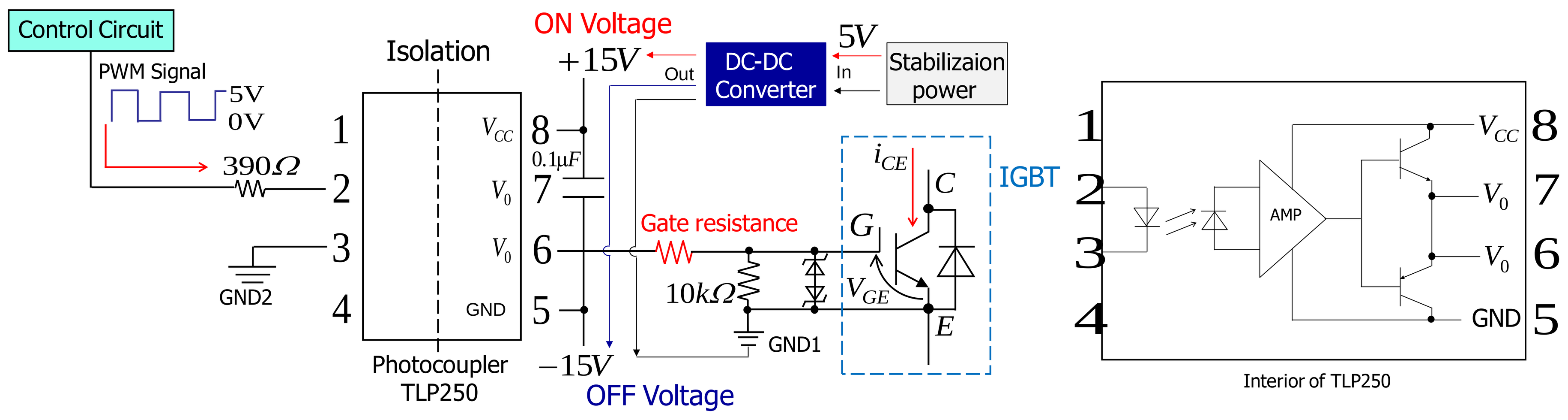

Fig.6. Principle of drive circuit

□Control circuit: low electric system
□Drive circuit: high electric system
} Isolation by photocoupler
□15V or-15V output by DC-DC converter

IGBT ON

ⅰ. PWM ON signal
ⅱ. 6 and 7 pin V_o=15V
ⅲ. V_{GE}=15V→IGBT ON
ⅳ. Start I_{CE}

IGBT OFF

ⅰ. PWM OFF signal
ⅱ. 6 and 7 pin V_o=-15V
ⅲ. V_{GE}=-15V→IGBT OFF
ⅳ. Stop I_{CE}

Experiment of chopper circuit

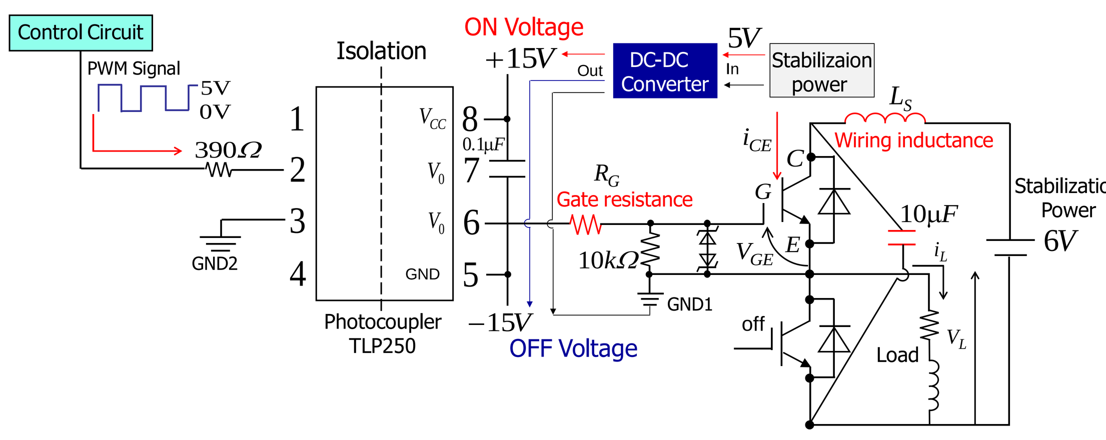

Fig.7. Experiment of chopper circuit

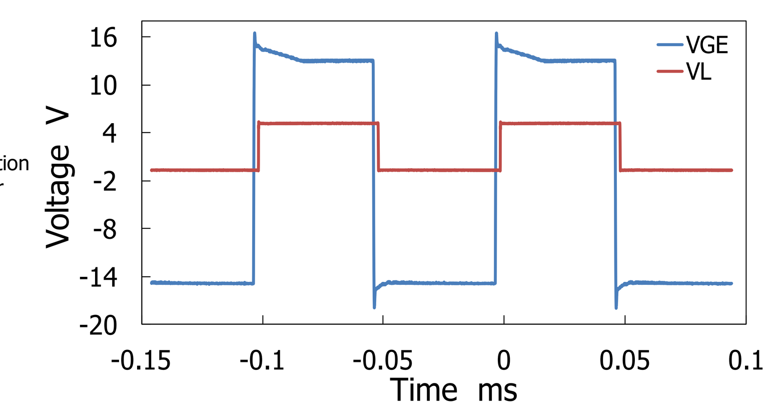

Fig.8. Response of V_L

□Confirmed response of V_L(Fig.8)
□Optimization of Surge voltage and switch speed

RG=15.6Ω,Shorter length of L_S,Insertion of capacitance

Fabrication of Drive circuit

□Fabrication of drive circuit by optimized value of chopper experiment(Fig.9)
□Check of fabricated inverter

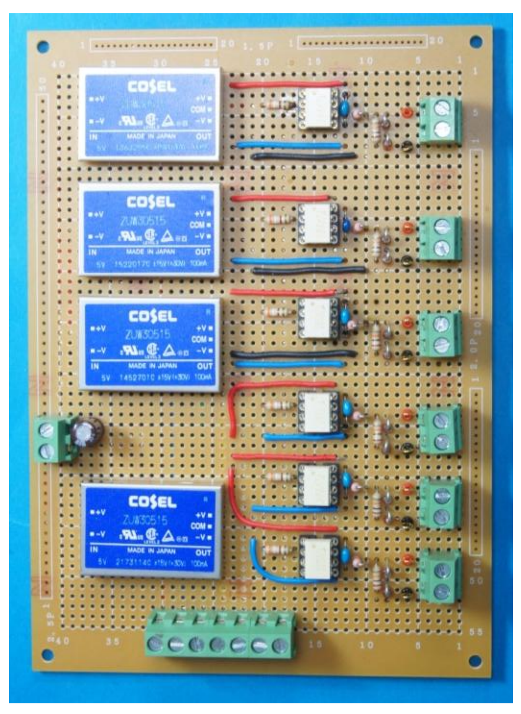

Fig.9. Fabricated Drive Circuit

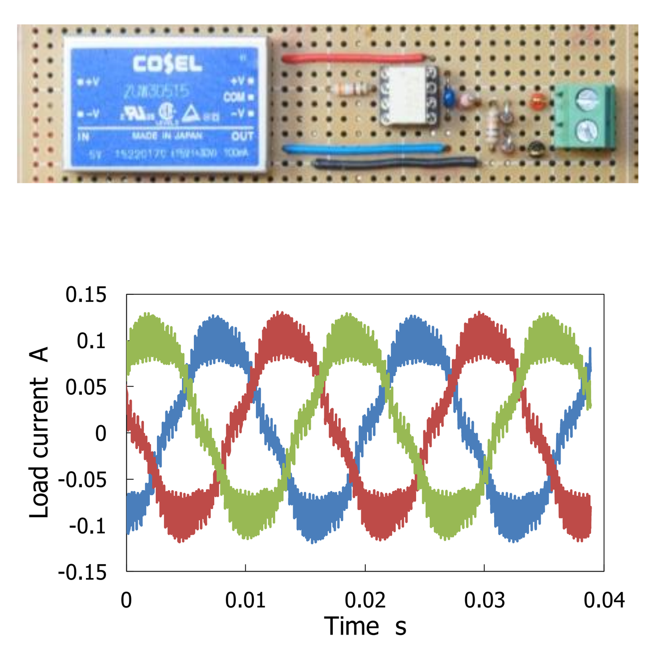

Fig.10. Confirmed Three Phase Wave

Conclusion

□Fabrication of inverter and its drive circuit
□Confirmed Three-phase wave